^{13}C NMR Determination of the Degree of Cocrystallization in Random Copolymers of Poly(β-hydroxybutyrate-*co*-β-hydroxyvalerate)

David L. VanderHart[†] and William J. Orts*[,‡]

Polymers Division and Reactor Radiation Division, National Institute of Standards and Technology, Gaithersburg, Maryland 20899

Robert H. Marchessault

Department of Chemistry, McGill University, 3420 University Street, Montreal PQ H3A 2A7, Canada

Received January 20, 1995[⊗]

ABSTRACT: A series of bacterially produced poly(β-hydroxybutyrate-*co*-β-hydroxyvalerate) copolymers containing random distributions of 3-hydroxybutyrate (3HB) and 3-hydroxyvalerate (3HV) were characterized by solid-state CPMAS ^{13}C NMR to determine the degree of cocrystallization of the two components. The 3HV minor component was shown to be incorporated into the poly(β-hydroxybutyrate)-type crystalline phase over the 3HV composition range of 0−27 mol %. The ratio of the 3HV content in the crystalline phase to the overall 3HV composition increases with increasing 3HV content, implying that it is easier to accommodate the larger 3HV residue in a crystalline region which already contains lattice imperfections. For samples with 3HV compositions of 21 and 27%, the 3HV content in the crystalline phase was roughly $^2/_3$ of the overall 3HV content. Asymmetric line broadening in the ^{13}C NMR spectra showed that the 3HV ethyl side branches assume multiple configurations when included in the crystalline phase. For the 27% 3HV sample, two different crystalline structures were detected—the poly(β-hydroxybutyrate) (PHB) and poly(β-hydroxyvalerate) (PHV) type lattice structures. The latter crystal structure is present despite the fact that the overall 3HV composition is below 40%, the composition at which the PHV-type crystal structure is generally formed. Both crystal types are formed because the 3HV content in the *noncrystalline* phase is above the changeover composition. The coexistence of PHV and PHB lattices suggests that there may also be a change in crystal composition as a function of crystallization time.

Introduction

Poly(β-hydroxybutyrate) (PHB) is a highly stereoregular biopolymer produced by many strains of bacteria as an energy storage medium.[1,2] The mechanical properties of this polymer along with its natural biodegradability sparked industrial interest in its production and utilization. Nevertheless, PHB tends to have problems with embrittlement and aging. Significant improvements in mechanical properties have been obtained by using relatively complex carbon sources to bacterially synthesize a wide range of these poly(hydroxyalkanoates) with the same backbone as PHB but with different side-chain constituents.[3,4]

Copolymers of 3-hydroxybutyrate with 3-hydroxyvalerate, P(3-HB−3HV), are presently the most likely of the poly(hydroxyalkanoates) to have a market impact (note that the polymer bonding is denoted as either a 3- or β-linkage). They are isotactic, random copolymers exhibiting a wide array of properties which vary with the copolymer composition. Bluhm *et al.*[5] first noted that there is significant cocrystallization of the minor-component residue in the host crystalline (CR) lattice. For compositions of 0−40% 3HV, P(3-HB−3HV) crystallizes in the PHB-type lattice with inclusion of the minor 3HV residues. To understand the composition/property relationship of P(3HB−3HV), one would like to know the degree of this cocrystallization. Moreover, the composition of the crystalline phase is not necessarily stable during the aging process. Partitioning of the minority residues in the host crystal lattice of the majority species has been dealt with for P(3HB−3HV) both theoretically[6] and experimentally.[7−13] While there is a general consensus that the concentration of the 3HV residues in a PHB-type lattice is lower in the CR region compared to the overall 3HV concentration, there is disagreement regarding the exact degree of partitioning. Using measurements of density, X-ray diffraction, and DSC, Sanchez Cuesta *et al.*[8] concluded that, in the range from 0 to 27 mol % 3HV, the concentration in the crystalline phase is about $^2/_3$ the overall concentration. On the other hand, reports based on line-shape analysis of the methyl region of ^{13}C CPMAS NMR spectra suggest either that there is a threshold somewhere between 18 and 31% 3HV below which 3HV residues are excluded from the crystalline phase[7] or that, for an 18.3 mol % 3HV sample, the concentration of 3HV in the CR regions is usually about 40% of the overall concentration.[9] Several research groups predict that the ratio of the 3HV composition in the CR phase to the overall 3HV composition will increase with increasing HV content up to 30 mol %.[6,10,11] To complicate this picture, the thermal history has a significant effect on such properties as the density[8,11] and the lamellar long period,[10−12] which can nearly double upon annealing. Despite significant changes in morphology, a reasonably consistent degree of crystallinity (55−68%) is maintained for samples crystallized at temperatures ranging from 20 to 115 °C.[10] Considering that the crystalline morphology of P(3HB−3HV) varies with thermal history and aging, it is quite conceivable that the partitioning will also vary.

In this paper, we examine random copolymers of 3-hydroxybutyrate-*co*-3-hydroxyvalerate P(3HV−3HV) by solid-state ^{13}C NMR to determine the crystallinities and the partitioning of the minor fraction residues of

[†] Polymers Division, NIST.
[‡] Reactor Radiation Division, NIST.
[⊗] Abstract published in *Advance ACS Abstracts,* August 1, 1995.

0024-9297/95/2228-6394$09.00/0

3HV into the CR PHB-type lattice. The range of 3HV composition studied is 0–27 mol %. The ^{13}C NMR method[14] used herein to separate the CR and noncrystalline (NC) components of the overall CPMAS spectrum is different from and, we believe, superior to the approach based on methyl line-shape analysis.[7,9] Our results also stand in contrast to those reported results. A limited amount of annealing data is also presented to examine the hypothesis that the level of incorporation of 3HV residues in the PHB lattice is a function of thermal history.

Experimental Section

Six samples were received from Imperial Chemical Industries, U.K.,[15] and analyzed by solid-state NMR. These bacterially produced biopolymers from *Alcaligenes eutrophus* are random copolymers with molecular weights ranging from 180 to 290K. The as-received samples had been originally precipitated from a chloroform solution using methanol,[15] which effectively "erased" the thermal history, and were then stored (and thus annealed) at room temperature for more than 5 years. The six samples were pure PHB along with random P(3HB–3HV) copolymers; copolymers are designated PHB/xV where x, the mole percent of valerate in the copolymers, takes values 4.4, 6.7, 16.9, 21, and 27. No special care was taken to dry the samples following our observation that, at 200 MHz, proton Bloch-decay spectra for as-received and 16-h-vacuum-dried (at room temperature) samples of PHB/27V were identical.

The NMR spectrometer used for ^{13}C spectroscopy is noncommercial and operates at 2.35 T (25.193 MHz for ^{13}C nuclei). Cross polarization (CP) techniques along with high-power decoupling and magic angle spinning (MAS) were combined in the usual way[16] to produce CPMAS spectra. CP times employed were 0.7 ms. The nutation frequencies corresponding to the radio-frequency (rf) field strengths were 66 and 69 kHz for carbons and protons, respectively, where the difference between these frequencies corresponded to the 3.2–3.5-kHz MAS frequencies. All spectra were taken at ambient temperature.

The strategy for isolating the spectrum corresponding to the CR phase of each sample has been presented previously[14] and is based on a two-phase model for the solid (CR and NC phases) and on the assumption that, during proton spin locking (SL), net proton polarization gradients are insignificant on distance scales of the monomers. Briefly, this method consists of taking spectra at different proton SL times prior to CP. During SL, proton polarization decays with a time constant, $T_{1\rho}^{H}$, the rotating-frame relaxation time. Owing to differences in molecular mobility between the CR and NC phases in these samples, relaxation takes place more rapidly in the NC compared with the CR phase. Consequently, the fraction of the total spectral intensity arising from the CR regions will increase as the spin-lock time increases. Hence, if one can recognize the spectral signatures of the two phases, one can isolate the spectra corresponding to each of the two phases by taking appropriate linear combinations of experimental spectra acquired with two SL times. This approach sometimes fails when the thinner dimensions of the phases are such that spin diffusion,[17] a polarization transport process, is capable of averaging the polarizations of the two phases on the time scale of the shorter of the intrinsic $T_{1\rho}^{H}$'s. Fortunately, this condition did not prevail for these materials.

An important assertion which motivates the effort to separate resonances representing the CR phase of PHB is that, owing to the presence of spin diffusion, the proton polarization level for a minority species, like 3HV, will be virtually identical to that of its surrounding PHB neighbors. Hence, a process which isolates the PHB CR signal automatically isolates the 3HV signals from that region. Over the copolymer composition range studied herein, the crystalline phase is that of PHB;[5] hence, 3HV residues in this phase are considered as defects.

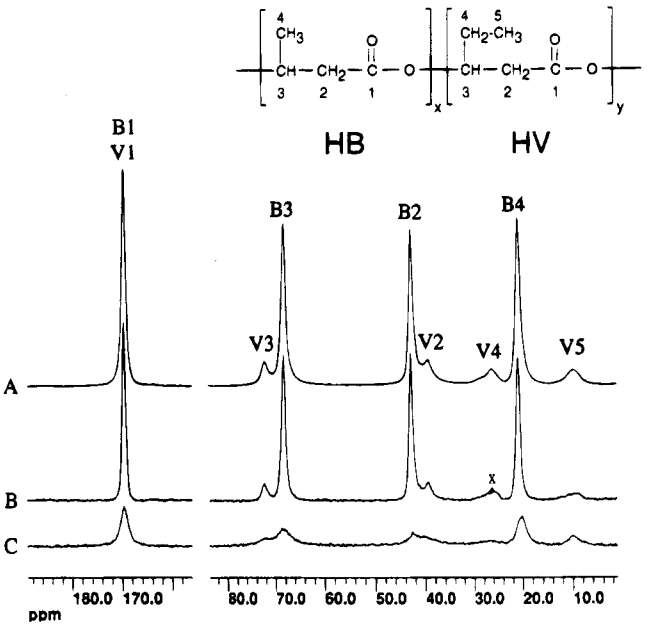

Figure 1. Ambient-temperature, 25-MHz CPMAS spectra pertaining to the PHB/21V sample. (A) Experimental CPMAS spectrum with 1-ms SL time; (B and C) synthesized spectra representing the crystalline (CR) and the noncrystalline (NC) phases, respectively. These spectra each consist of different linear combinations of A and a spectrum (not shown) having 5 ms of SL prior to the 0.7 ms of CP common to all spectra. Spectrum A is exactly the sum of B and C. The "X" marks the position of the carbonyl spinning sideband in B, and the blackened area approximates the contribution of this sideband. (See the text for criteria applied in generating the synthesized spectra.) The polymeric repeat units of 3HB and 3HV are represented in the chemical structure, and the corresponding resonances in this random copolymer are indicated by the B and V labels, respectively.

Results and Discussion

The objectives of this NMR investigation were as follows: first, we wished to verify by different methods than those employed previously[5,7–10] that 3HV residues are found in the CR regions of the copolymers for compositions 0–27 mol % 3HV. Second, we sought to offer our best quantitative estimate of the mole fraction of the 3HV residues in the CR regions. In so doing, we test whether the 3HV concentration in the CR regions is a linear function or nonlinear function of the overall 3HV composition (the results of Kamiya *et al.*[7] imply nonlinearity). Third, we sought to provide a qualitative comment on whether the 3HV residues associated with the CR regions are mainly concentrated at the CR/NC interface or spread uniformly through the CR phase.

The experimental data along with our line-shape analysis are presented first, followed by discussions of the validity of the assumptions used during analysis. Figure 1 is a set of spectra pertaining to the PHB/21V sample. Spectrum A is the only experimental spectrum shown; it is the CPMAS spectrum taken with 1-μs SL and 0.7-ms CP time. Spectrum B is that of the CR phase, and spectrum C is that of the NC phase. These latter spectra are generated from linear combinations of spectrum A with an experimental spectrum (not shown) taken at some longer SL time, usually 15 ms. Table 1 gives the relative amplitude changes for the signals from each phase at the indicated SL times. The procedure for producing these spectra is as follows: first, the spectrum of the CR phase is generated using the notion that the sharper spectral features are associated with the CR phase[18] and using the criterion that, in

Table 1. Amplitude Ratios, R(CR) and R(NC), of the NMR Signals from the CR and NC Regions of the P(3HB−3HV) Copolymer Samples at the Given Spin Locking (SL) Times,[a] Referenced to the Amplitudes at 1 μs of SL

sample	SL time (ms)	R(CR)	R(NC)	R(NC)/R(CR)
PHB/0V	15	0.81	0.55	0.68
PHB/4.4V	15	0.74	0.36	0.48
PHB/6.7V	15	0.72	0.31	0.43
PHB/16.9V	15	0.59	0.20	0.34
PHB/21V	2	0.97	0.70	0.72
	5	0.88	0.50	0.57
	12	0.67	0.34	0.51
	15	0.60	0.30	0.50
	25	0.40	0.20	0.50
PHB/27V	15	0.65	0.18	0.28
PHB/27V	15	0.64	0.20	0.31

[a] Several SL times were used for the PHB/21V sample in order to investigate the possibility of a high concentration of PHV residues at the CR/NC interface.

isolating these features, no negative intensity is permitted. In these spectra, the line widths for carbons in the CR phase are narrow enough with respect to those in the NC phase that there is little room for subjectivity in applying this method. Then, the spectrum of the NC phase is generated by appropriately scaling line shape B and subtracting it from spectrum A using the criterion that no negative-going "wedges" should be hollowed out of the resulting line shapes in the positions of the "CR-carbon" resonances. Thus, spectrum A is exactly the sum of spectra B and C, even though each of the latter spectra are different linear combinations of two experimental spectra.

The foregoing method may seem antiquated and clumsy in a day when one can use computers to deconvolute line shapes into various components. However, there is reasonable spin physics in this method; moreover, we cannot assume *a priori* that CPMAS line shapes will adhere to a certain mathematical shape. We will see presently that some of the 3HV resonances in the CR phase have very obviously unsymmetrical resonance shapes.

The assignment of the various carbon resonances has been published previously,[5] and these assignments, referenced to the polymer structure, are included in Figure 1. The minor feature near 26 ppm, marked with an "X" and blackened in Figure 1B, is the spinning sideband of the carbonyl resonance. It is clear in B that the ethyl branch resonances, V4 and V5, and the methine backbone resonance, V3, are the best resolved from the resonances of PHB. The quantitative analysis of the fraction of 3HV residues in the PHB CR region focuses on this methine region because (i) the motion of the backbone methine carbon ought to be very limited in the CR region with the result that reasonable resolution and predictable, fast CP rates for both the V3 and B3 resonances over the 0.7 ms of CP ought to prevail and (ii) V3 and B3 resonances are reasonably symmetric and quite well resolved so that relative intensities may be determined quite accurately.

Using the method illustrated in Figure 1 and the data from Table 1, we were able to generate CR spectra for all six samples (see Figure 2). Corresponding results are given in Table 2. The mole fractions of the 3HV residues in the CR regions, X_{vC}, are obtained by integration, after line-shape deconvolution of the two OCH peaks. The possibility that this method will give misleading results is quite remote since CP techniques become more quantitative as solids become more rigid and as $T_{1\rho}^{H}$'s increase.

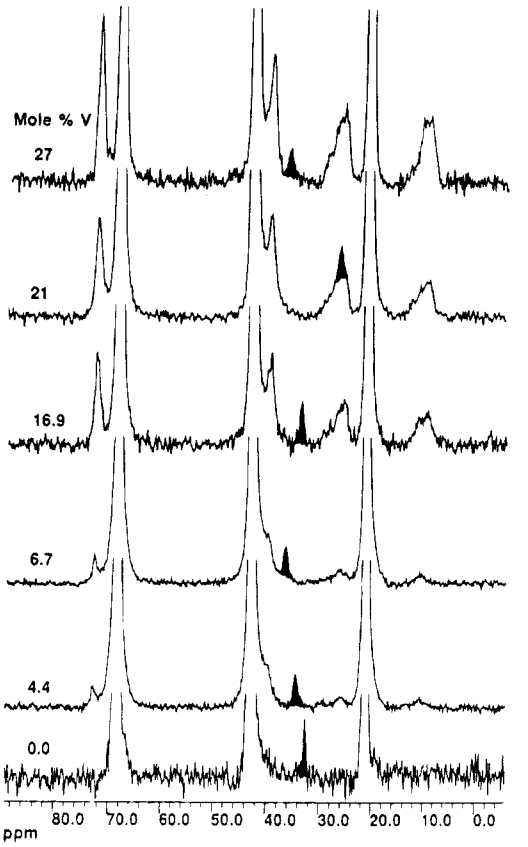

Figure 2. Aliphatic region of ^{13}C line shapes, isolated in the manner illustrated in Figure 1, corresponding to the crystalline regions (CR) of the samples indicated. These spectra are all normalized to the same total intensity; hence, the integrals of the V3 resonance near 73 ppm are proportional to the mole fraction 3HV in the CR regions. Spinning sidebands of the carbonyl resonance are darkened. Noise levels are a function of the number of scans and the R(CR) and R(NC) values of Table 1.

Table 2. Crystalline Fractions,[a] Line Widths for the OCH Carbons in the Crystalline Regions,[b] and Mole Percents[c] PHV in the Crystalline and Noncrystalline Phases of the P(3HB−3HV) Copolymers

sample	f_c	B3 LW	V3 LW	X_{vC}	X_{vNC}
PHB/0V	0.53	0.56			
PHB/4.4V	0.58	0.60	*d*	0.016 ± 0.004	0.08 ± 0.01
PHB/6.7V	0.58	0.62	0.70	0.023 ± 0.004	0.13 ± 0.01
PHB/16.9V	0.57	0.85	1.10	0.097 ± 0.010	0.26 ± 0.02
PHB/21V	0.60	0.97	1.30	0.119 ± 0.011	0.34 ± 0.03
PHB/27V	0.65	0.95	1.17	0.200 ± 0.012	0.38 ± 0.04
PHB/27V(ann.)	0.56	0.92	1.20	0.184 ± 0.009	0.40 ± 0.03

[a] Based on the deconvolution of the CPMAS line shapes illustrated in Figure 1. Minor (<0.03) corrections for the unequal $T_{1\rho}^{H}$ decays in the two phases during the 0.7 ms of CP have been applied; however, no correction has been made for any differential carbon relaxation to the lattice during CP. [b] Full width at half-height, in ppm, of the OCH line width near 69 ppm in the middle spectra of Figures 1−3; OCH-B and OCH-V refer to the 3HB and 3HV resonances, respectively. [c] Mole fractions in the crystalline phase are obtained by integration of the two peaks in the OCH spectral regions of spectra B in Figures 1 and 3. Mole fractions in the NC phase are calculated on the basis of the f_c and X_{VC} values and the known overall concentration of 3HV residues. [d] The signal is too weak to determine the line width accurately.

The apparent CR fraction in the CP spectra with 1-μs SL time, as shown in Figure 1, can be calculated using the relative OCH peak intensities of the middle, relative to the upper spectra. However, the overall crystallinity of a sample, f_c, is generally different from the apparent CR fraction calculated at a given spin-lock time, due, in part, to the preferential decay of the proton polariza-

tion in the NC relative to the CR regions. For example, we know that, during the finite CP time of 0.7 ms, the proton polarization has decreased more in the NC than in the CR region. Furthermore, the shorter the $T_{1\varrho}^{H}$ becomes in the NC phase, relative to the $T_{1\varrho}^{H}$ in the CR phase and relative to the 0.7 ms of CP, the larger this difference becomes. To make a reasonable estimate of the significance of this effect, we varied the spin-lock times for the PHB/21V sample and estimated the intrinsic $T_{1\varrho}^{H}$'s. From the trend in the data in Table 1 for the PHB/21V sample, one can see that the $T_{1\varrho}^{H}$ in the NC phase is shorter than that in the CR phase, as expected. From the data at several SL times, we determined that the intrinsic $T_{1\varrho}^{H}$ [19] in the NC region is 5.5−6 ms. The correction for the preferential decay of proton polarization in the NC region thus gives an overall crystallinity of 0.60 instead of the apparent value of 0.63 based solely on the fractional contribution of spectrum B to spectrum A.

One cannot make as precise a correction to the apparent crystallinities of the other samples since only two SL times were used. That is, when spin diffusion is active between the CR and NC protons during SL, both decays are nonexponential and one cannot extract the intrinsic $T_{1\varrho}^{H}$'s of each region from the amplitudes at just two SL times. Thus, the CR fractions appearing in Table 2 have been obtained by reducing their apparent fractions, by 0.03 for all of the copolymers and by 0.02 for PHB, to approximate the $T_{1\varrho}^{H}$ corrections. Since these corrections are relatively small and since the crystallinity of the samples is not regarded as critical to this study, we decided not to measure the NC decay rates over a wide range of SL times for all the samples. In principle, one can also get crystallinities from Bloch decay spectra, provided one waits sufficiently long for full carbon recovery between scans. We performed such experiments on the PHB/21V sample using 100-s delays between scans. The inferior signal-to-noise ratio in these spectra, relative to the CPMAS spectra, allows us only to say that the CPMAS and Bloch decay MAS line shapes looked the same in the OCH region where the analysis was performed. Certain line-shape differences showed up in the methyl region owing to slower CP rates and possibly other motion-related complications for this kind of carbon. Thus, we feel quite confident in the f_c values. There is also a reasonable agreement between these f_c values and those determined from X-ray analysis on these samples.[5,10,20] A knowledge of f_c and X_{vC} leads directly to a determination of X_{vNC} given in Table 2.

One assumption implicit in this method is that samples consist of two phases, CR and NC, and that there is a uniform distribution of 3HV residues in each of the two phases. This raises the question, namely, can one obtain any experimental evidence that a higher concentration of 3HV residues exists at the CR/NC interface? On the basis of qualitative arguments, we offer experimental evidence that the 3HV units in the CR region are not highly concentrated near the interface. This assertion stems from the fact that the linear-combination "CR" spectra for the PHB/21V sample generated with different pairs of experimental spectra (for both mathematical and signal-to-noise purposes always including the spectrum with 1-μs SL) result in a consistent concentration of 3HV residues in the CR phase. The process of spin diffusion generates a steady-state profile of polarization after a time on the order of 10 ms for the PHB/21V sample (see Table 1). Prior to achieving this steady state, the ratio of polarization at the interface to the average CR polarization is a changing function. If there were a high concentration of 3HV monomers near the interface, the CR spectrum arising from the combination of the 1-μs SL/2-ms SL spectra would show a different level of 3HV incorporation than the CR spectrum arising from the 1-μs SL/15-ms SL pair. It was found that these CR spectra were the same. Clearly, this test is only meaningful when one uses spectra with SL times where the ratio, R(NC)/R(CR), shows contrast between runs (see Table 1). Thus, we concluded that there is not a high concentration of 3HV residues at the interface. This is consistent with a model of P(3HB−3HV) put forth by Bluhm *et al.*[20] from analysis of small-angle X-ray scattering data that the crystalline morphology is better described as consisting of two distinct phases, CR and NC, rather than having a significant CR/NC interfacial region. We note, however, that the proof of rigorous concentration uniformity throughout each phase requires stronger support than we have given here.

There is another observation which is consistent with a reasonably uniform distribution of 3HV residues throughout the CR region. The data in Table 2 indicate that the line widths of the CR phase for both 3HV and 3HB is a steadily increasing function of 3HV concentration. If the 3HV residues were confined mostly to the surface of the crystals, it would seem reasonable that the average methine line widths of the CR 3HB and 3HV residues would be more disparate than is seen (Table 2) since the 3HV residues would then be concentrated in regions of higher disorder.

We can also draw a qualitative conclusion about the uniformity of 3HV conformations at the defect sites within the CR phase. From spectra B and C we see that the 3HV backbone resonances near 70 ppm are reasonably symmetrical and clearly narrower in the CR phase than in the NC phase (although, not surprisingly, the line widths in Table 2 at the OCH position for the 3HV residues are slightly larger than those for the corresponding PHB residues, which fit well into the lattice). However, in spectrum B and in those of Figure 2, the ethyl branch resonances, V4 and V5, are asymmetric and have line widths of 2.5−3 ppm. Hence, it would follow that there is considerably more disorder for the 3HV ethyl branch carbons in the CR phase than there is for the 3HV backbone carbons. (This conclusion had also been reached previously[5] although not in the context of having separated the spectrum of the CR region.) This disorder can be positional and/or dynamic; however, since dynamic contributions lead to symmetric broadening, the asymmetry of these branch resonances suggests that a substantial component of the disorder is positional. We speculate that this positional disorder is not primarily a function of having numerous defects in the CR regions since, in Figure 2, the widths of the resonances associated with the methyl carbon are not sensitive to 3HV concentration. This disorder may stem from more than one conformation of the ethyl branch in the CR. For example, in studies of the α- and β-crystalline forms of P(3HB−3HV), several groups[21,22] have implied that multiple conformations of the ethyl branch are possible with reasonably small energy costs.

Several conclusions can be derived from the data in Table 2. First, it is clear that the 3HV residues are incorporated into the CR phase. Second, the ratio of the concentration of 3HV residues in the CR phase to the overall concentration of 3HV residues is not linear

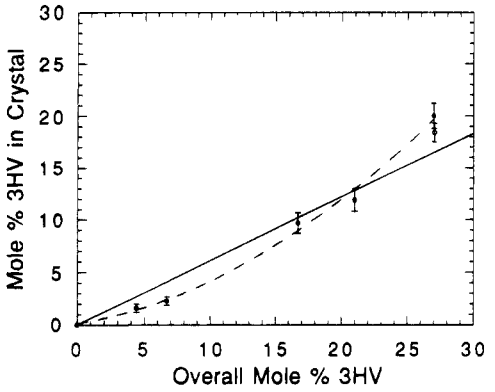

Figure 3. Plot of the mole percent 3HV residues in the CR region versus the overall mole fraction 3HV. The two lines are best fits, linear and quadratic in the overall mole fraction, constrained to pass through the origin. The functional form of the quadratic curve, an acceptable fit, is strictly empirical.

but goes from about 0.35 in the PHB/4.4V and PHB/6.7V samples up to about 0.67 in the PHB/27V sample. Figure 3 is a plot of the mole percent 3HV in the CR regions versus the overall 3HV mole percent. The best linear fit to this data (constrained to go through the origin) falls outside of experimental error. The curved line in Figure 3 is an empirical fit—second order in the overall 3HV concentration—and is also constrained to pass through the origin. (This fit need not be the true functional dependence.) Clearly, there is a tendency to exclude the defects from the CR regions at low 3HV compositions. As the relative number of defects in the CR increases, there is a greater tendency to include a larger fraction of 3HV residues. This is reasonable considering that it should be easier to add the excess volume necessary for a defect into an already imperfect lattice, as opposed to adding it into a defect-free lattice. This trend is consistent with DSC data,[5,12] where the heat of fusion is seen to diminish in this composition range as the 3HV composition rises.

Our results agree in the broad sense with previously published solid-state NMR studies on P(3HB−3HV) cocrystallization,[7,9] showing that there is substantial incorporation of 3HV into the PHB lattice. However, the degree of incorporation of 3HV residues in the PHB lattice reported here differs from the two previous studies due to significant differences in the method of analysis and, to a lesser extent, due to the effect of thermal history. Kamiya *et al.*[7] saw no incorporation of 3HV into the PHB crystals until the overall 3HV composition exceeded 18 mol %. Our results show incorporation of 3HV residues in the CR regions over the entire range from 4.4 to 27 mol %. The magnitude of incorporation of the minor component is significantly higher than those observed by Kamiya *et al.*[7] but more in line with the results of Yoshie *et al.*,[9] who reported that, at an overall 3HV composition of 18.3%, the composition in the CR regions ranged between 7.0 and 10.9% depending on thermal history.

In recognition that the CP spectra we obtained for PHB/16.9V and PHB/21V look fairly similar to the spectrum obtained by Kamiya *et al.*[7] for their PHB/18.3V sample, we conjecture that our differences arise mainly in the assumptions going into our respective NMR analyses. In both previous NMR studies,[7,9] the asymmetric methyl resonances of dipolar-decoupled (DDMAS) NMR spectra were used to determine the degree of cocrystallization. These *asymmetric* peaks were modeled as two chemically-shifted overlapping

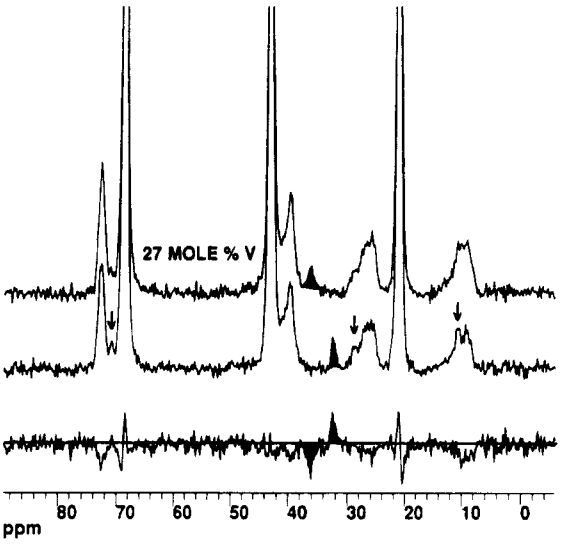

Figure 4. Aliphatic-region spectra of the CR domains corresponding to the PHB/27V sample. As-received (top), annealed for 16 h at 84 °C (middle), and difference (middle − top). Spectra are normalized to the same PHB-resonance amplitudes. Note that annealing has resulted in a small decrease of the 3HV concentration, a possible splitting of the V5 methyl peak, very small shifts in opposite directions for the B4 and B3 peaks, and the appearance of a small resonance at about 70.8 ppm, associated with 3HV residues in a PHV lattice.

symmetric peaks corresponding to the amorphous and crystalline contributions. From the CR spectrum shown in Figure 2, one can clearly question the validity of this assumption, since, as discussed above, the crystalline 3HV methyl resonances are not simple symmetric peaks. We stress again that the fundamental conditions which must be met to isolate the CR spectra[14] have been met for the P(3HB−3HV) copolymers, i.e., (i) that the $T_{1\varrho}{}^{H}$'s in the CR and NC regions are sufficiently different, (ii) that the line widths for the CR and NC regions have good contrast, and (iii) that the CR and NC domains are correspondingly large to permit the extraction of the resonance shape of the CR regions.

There are clear differences in the thermal history of samples between this study and the previous NMR studies.[7,9] Whereas Kamiya *et al.*[7] and Yoshie *et al.*[9] melt-crystallized their samples and allowed them to anneal for 5 days, we recorded spectra from "as-received" samples. Our samples were initially crystallized out of solution using a nonsolvent more than 5 years ago and then allowed to anneal at room temperature. We chose to work on such samples in an attempt to study an "equilibrium" sample. Room-temperature aging in P(3HB−3HV) is a recognized[23] phenomenon, albeit it is not well understood. One surmises that there is some development of crystallinity which accompanies this aging, since, for example, elongation to break is a decreasing function of aging time.

Although thermal history seems to affect the degree of partitioning,[9] it does not account for the significant differences between our results and those of the previous studies.[7,9] To test this, we obtained spectra from the PHB/27V sample annealed *in vacuo* at 89 °C for 1 h followed by annealing at 84 °C for 16 h. The melting point of this sample is approximately 100 °C.[14] The CR spectra of this sample, before and after annealing, are shown together with the difference spectrum in Figure 4. The measured X_{vC} from these spectra decreased only modestly from 0.200 to 0.184 upon annealing. In fact, within the liberal limits of uncertainty given in Table

2, there is no significant change with annealing. However, the negative intensities in the regions of the 3HV resonances in the difference spectrum give reasonable indication that the 3HV concentration has been reduced upon annealing. This small reduction in X_{vC} is accompanied by a decrease in crystallinity from 0.65 to 0.56. We considered, though, that the sample had not reached its full degree of crystallinity. The annealed sample was investigated again 5 days after annealing, with no visible change in crystallinity or partitioning.

It is noteworthy that in the PHB/27V sample the calculated X_{vNC} is near 0.40—the composition where one would expect the crossover from the PHB to the PHV crystalline lattice. One can consider crystallization to be a process during which the NC regions become richer in 3HV residues by virtue of partitioning.[6] If the 3HV concentration in the NC phase becomes high enough, it is conceivable that nucleation and growth of some PHV-lattice crystals would occur. The PHV lattice would correspond to lines appearing near 10.8, 28.9, and 70.8 ppm.[5] The spectra in Figure 4, both before and after annealing, show weak features at these positions. These resonances are more obvious in the annealed sample owing to better signal-to-noise. Thus, a small amount of PHV-lattice crystals has formed, reenforcing the idea that crystal composition changes with crystallization time. This is in keeping with DSC data, where melting endotherms are broader with increasing mole percent 3HV from 0 to 40 due to a spread in the number of defects and/or crystallite size.[12,14] Our NMR data are not sensitive to such an accompanying distribution in partitioning, and the numbers given herein should be regarded as averages.

It is interesting to speculate on the kinetics of crystallization in determining the degree of partitioning. If one were to cool, say, the PHB/27V sample very slowly from the melt, the first nuclei to form would have a rather low defect concentration, since the melting point decreases with increasing 3HV in the composition range 0−40 mol % 3HV, and these nuclei have the greatest undercooling. Once the nuclei are stable, it is conceivable that further crystallite growth may include stems with higher concentrations of 3HV. As cooling progresses, nuclei with increasing numbers of defects would form and subsequent crystal growth would occur (late-forming nuclei could include those having the PHV lattice). Hence, in the limit of very slow cooling from the melt, there would be a distribution of the average defect content both within and among crystallites which depends on the kinetics of crystallization.

The preceding picture of crystallization is oversimplified since it ignores chain connectivity and entropic issues. Such considerations, which would act to reduce the partitioning during crystallization, include the following: (i) The interface at which stems make the transition from CR to NC is an area where density considerations cause many chains to fold tightly on themselves.[24] Since the range of 3HV content per stem length decreases as the stem length increases, a truly tight fold would effectively double the stem length and move the 3HV content in the crystal in the direction of the overall 3HV content. (ii) It has been previously observed that, at a given crystallization temperature, the stem length (or long period) increases with increasing defect composition.[10,25] For example, the long periods measured by X-ray for PHB/21V and PHB crystallized at 115 °C are 22.0 and 11.4 nm, respectively.[10] Presumably the longer stem length is a result of crystal thickening due to a smaller undercooling as the 3HV content increases (up to 40%). The longer stem length again moves the average stem composition closer to the overall composition. (iii) Finally, if one considers that the average molecular weight of these chains is 250K and an average stem length assuming no chain tilt is roughly 8 nm, there are roughly 200, "stem lengths" per chain. For 60% crystallinity, 120 of these stems are eventually crystallized. With this many stems involved in crystallization, one would not expect to be able to select all of the 120 stems of lowest defect content into crystalline regions, owing to the fact that, as lower-defect stems become incorporated into growing crystals, the translational freedom of the remaining stems would become very restricted, especially in the late stages of crystallization.

Summary

CPMAS ^{13}C NMR has been used to determine the degree of cocrystallization of poly(3-hydroxybutyrate-*co*-3-hydroxyvalerate), P(3HB−3HV), in the 3HV composition range 0−27 mol %. A significant fraction of the 3HV minor components are incorporated into the PHB-type CR phase. The ratio of the 3HV content in the CR phase to the overall 3HV composition increases with increasing 3HV content, implying that it is easier to insert a defect into a CR phase which already contains defects. For the PHB/21V and PHB/27V samples, roughly $^2/_3$ of the 3HV residues are accommodated in the CR phase. This value is in agreement with the results of Sánchez Cuesta *et al.*[8] determined by combining measurements from X-ray scattering, DSC, and density.

The ^{13}C spectra contain several peak asymmetries which are indicative of two notable phenomena. First, the lines corresponding to the crystalline 3HV ethyl side branches are asymmetric and broad, implying that the longer 3HV branch assumes more than one configuration when it is included as a defect. Second, and perhaps more noteworthy, in the spectra from the PHB/27V sample, there are lines indicative of the PHV-type crystal lattice. Formation of the PHV crystal structure ties in with the fact that the 3HV content in the noncrystalline phase is near 40%, the composition at which one expects a change in crystal structure. Thus, there is a spread in crystallite population, varying not only in size and defect content but also in crystal structure.

There is qualitative experimental support that the defects in the PHB-type CR phase are not grouped near the crystalline/noncrystalline interface. Such information is critical in modeling the crystalline morphology and the kinetics of crystallization. On the basis of the lengths of the crystalline stems in the CR phases, the high degree of crystallinity (55−65%), and the entropic limitations of chain conductivity, we argue that thermal history should have a limited effect on the degree of cocrystallization of P(3HB−3HV) random copolymers.

References and Notes

(1) Merrick, J. *Photosynth. Bact.* **1978**, *199*, 219.
(2) Dawes, E. A. *Microbial Energetics*; Blackie: Glasgow, U.K., 1986.
(3) Witholt, B.; Lageveen, R. G.; Huisman, G. W.; Preusting, H.; Nijenhuis, A.; Kingma, J.; Tijsterman, A.; Eggink, G. *Polym. Prepr. (Am. Chem. Soc., Div. Polym. Chem.)* **1988**, *29*, 592. Lageveen, R. G.; Huisman, G. W.; Preusting, H.; Ketelaar, P.; Eggink, G.; Witholt, B. *Appl. Environ. Microbiol.* **1988**, *54*, 2924.

(4) Lenz, R. W.; Kim, B.-W.; Ulmer, H. W.; Fritzshce, K. In *Novel Biodegradable Polymers*; Dawes, E. A., Ed.; Kluwer: Dordrecht, The Netherlands, 1990; p 23.
(5) Bluhm, T.; Hamer, G. K.; Marchessault, R. H.; Fyfe, C. A.; Veregin, R. P. *Macromolecules* **1986**, *19*, 2871.
(6) Kamiya, N.; Sakurai, M.; Inoue, Y.; Chûjô, R. *Macromolecules* **1991**, *24*, 3888.
(7) Kamiya, N.; Sakurai, M.; Inoue, Y.; Chûjô, R.; Doi, Y. *Macromolecules* **1991**, *24*, 2178.
(8) Sánchez Cuesta, M.; Martínez-Salazar, J.; Barker, P. A.; Barham, P. J. *J. Mater. Sci.* **1992**, *27*, 5335.
(9) Yoshie, N.; Sakurai, M.; Inoue, Y.; Chûjô, R. *Macromolecules* **1992**, *25*, 2048.
(10) Orts, W. J.; Marchessault, R. H.; Bluhm, T. L. *Macromolecules* **1991**, *24*, 6435.
(11) Barker, P. A.; Mason, F.; Barham, P. J. *J. Mater. Sci.* **1990**, *25*, 1952.
(12) Barham, P. J.; Keller, A.; Otun, E. L.; Holmes, P. A. *J. Mater. Sci.* **1984**, *19*, 2781. Mitomo, H.; Barham, P. J.; Keller, A. *Sen-i Gakkaishi* **1986**, *42*, 589.
(13) Bloembergen, S.; Holden, D. A.; Hamer, G. K.; Bluhm, T. L.; Marchessault, R. H. *Macromolecules* **1986**, *19*, 2865.
(14) VanderHart, D. L.; Pérez, E. *Macromolecules* **1986**, *19*, 1902.
(15) Holmes, P. A.; Wright, L. F.; Collins, S. H. Eur. Pat. Appl. 0 052 459, 1982; Eur. Pat. Appl. 0 069 497, 1983. Certain commercial material and equipment are identified in this paper in order to specify adequately the experimental procedure. This in no way implies recommendation or endorsement by the National Institute of Standards and Technology.
(16) Schaefer, J.; Stejskal, E. O.; Buchdahl, R. *Macromolecules* **1975**, *8*, 291.
(17) Abragam, A. *Principles of Nuclear Magnetism*; Oxford University Press: London, 1961; Chapter V.
(18) VanderHart, D. L.; Earl, W. L.; Garroway, A. N. *J. Magn. Reson.* **1981**, *44*, 361.
(19) Kenwright, A. M.; Packer, K. J. *J. Magn. Reson.* **1986**, *69*, 426.
(20) Bluhm, T. L.; Orts, W. J.; Marchessault, R. H. In *Advances in X-ray Analysis*; Barrett, C. S., Ed.; Plenum Press: New York, 1992; Vol. 35, p 645.
(21) Orts, W. J.; Marchessault, R. H.; Bluhm, T. L.; Hamer, G. K. *Macromolecules* **1990**, *23*, 5370.
(22) Nakamura, K.; Naoko, Y.; Sakurai, M.; Inoue, Y. *Polymer* **1994**, *35*, 193.
(23) Orts, W. J. Ph.D. Thesis, Department of Chemistry, University of Toronto, Toronto, Ontario, Canada, 1990.
(24) Di Marzio, E. A.; Guttman, C. M. *Polymer* **1980**, *21*, 733.
(25) Sanchez, I. C.; Eby, R. K. *Macromolecules* **1975**, *8*, 638. Sanchez, I. C.; Eby, R. K. *J. Res. Natl. Bur. Stand., Sect. A* **1973**, *77*, 353.

MA950062N